NUMERICAL SIMULATION OF COMPOSITE CAR SEAT CUSHION

PAVEL SRB, MICHAL PETRU

Institute for Nanomaterials, Advanced Technologies and Innovation, Technical University of Liberec,

Liberec, Czech Republic

pavel.srb@tul.cz

Reduction of energy consumption, improving performance and efficiency is one of the most important factors influencing current trends in the development of components used in the transportation and automotive industry. For car producers, one of the possible ways of achieving such a goal is to reduce the weight of individual components while maintaining or improving the material properties during practical application. Therefore, the requirement of weight reduction also applies to car seat cushions. The use of low-density composite foams using fibrous reinforcements is a suitable solution. These materials have strong nonlinear viscoelastic behavior which is time dependent. Due to the synergistic effect of foam reinforcement, it is possible to reduce weight while maintaining the corresponding mechanical properties. In this study numerical simulations were used for analysis and design of the seat cushion with PU foam and composite foam and their results were evaluated. Mechanical properties of PU foam and composite foam are influenced by internal and external structure, shape and size of the cells, volume of the filling material and properties of the used polymer. Mechanical properties e.g. contact pressure, stress distribution and the dependence of stress on the strain rate are investigated.

KEYWORDS

numerical simulation, car seat, composite foam, natural fibers, low-density

1   INTRODUCTION

Automotive industry is imposing very high demands on the development of energy efficient components. One of the most important parameters is the low weight associated with lower emissions. An important component of the car is also the seat material. The car seat consists of many parts. One of them is a comfortable cushion. Despite its lower density, there is also an effort to reduce weight and price with the same level of comfort. By optimizing the cushion by following the shape of the human body, the cushion weight can be reduced by up to 50% with the same static comfort [Kamp 2012]. Key parameters to compare the characteristics of the car seat are the comfort and safety of the passenger. Reducing the weight of a car can be solved through changes in design of various components. The design of the car seat is significantly influenced by human anatomy. Each individual and his anatomy are associated with the comfort of a given space, which affects the easy accessibility of the car's controls. The weight and structure of the human body affects the interaction of the body and the seat, with the described distribution and contact pressure. Furthermore, it affects the dynamic parameters described by varying stiffness and damping, or the resulting transmissibility characteristics of the seat. These and other mechanical parameters depend on the shape and size of the contact surface of the compressed seat cushion. It has been discussed in a number of papers that the mechanical vibrations due to the dynamic forces generated by road and / or off-road driving, have adverse effects on humans. These vibrations are transmitted through the seat frame while driving [Griffin 2004, Fahy 2015, Valentini 2012]. Another desirable feature in reducing the weight of a car seat is maintaining or improving attenuation and minimizing mechanical vibrations transmitted to human body. Currently, the unresolved problem is the replacement of the material of seat cushion itself. The requirements for the seat cushion are very high, namely specific non-linear mechanical properties, ecology and recycling possibilities and low energy intensity of production. The solution could be not only in the modification of the geometry and the anatomical design of the seat, but also in the change of the car seat material which is not so dependent on the strain rate as PU Foam [Petru 2017]. By replacing the PU foam completely, the problem is not solved quickly and satisfactorily. The existing technological processes and production equipment would have to be discontinued. The use of low-density composite foams using fibrous reinforcements is therefore a desirable solution. Due to the synergistic effect of foam reinforcement, it is possible to reduce weight while maintaining the corresponding mechanical properties.

2   MECHANICAL PROPERTIES OF PU FOAM

These days, PU foam is widely used as filling material of car seat, as their production is relatively fast and accurate. Different shapes can be achieved in a relatively short time, according to the mold design. For the production of PU foam, a chemical mixture of isocyanate and polyol is used which reacts to form PU foam at relatively low pressure. PU foam is characterized by viscoelastic properties combining the properties of solid and liquid. Elastic properties predominate in short-term loading. Conversely, in long-term loading, it behaves similar to a viscous liquid [Szycher 2017]. PU material is characterized by its strongly non-linear behavior [Kanoko 2020, Marvi-Mashhadi 2020]. When compressing a sample, the force response is dependent on both the value and the rate of deformation. The hysteresis curve is formed by the stress dependence on the deformation of the material being compressed and unloaded. When the foam is compressed, the walls of the foam cells are deformed. On subsequent unloading, the relief is restored to the original shape. Long-term loading results in two significant events due to viscous behavior. In the case of permanent deformation, the pores are deformed and are unable to regenerate sufficiently quickly.
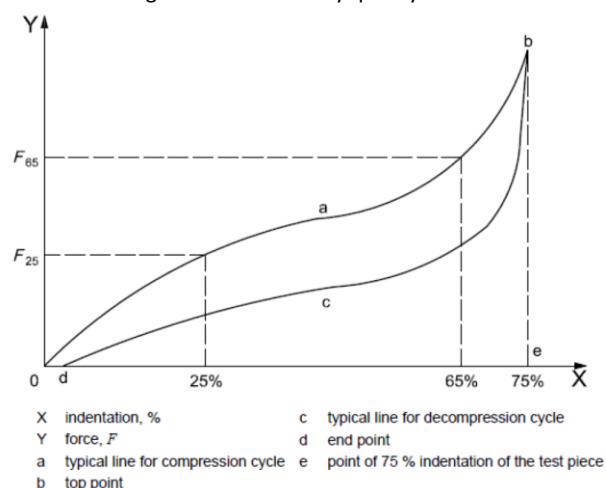

X	indentation, %	c	typical line for decompression cycle
Y	force, F	d	end point
a	typical line for compression cycle	e	point of 75 % indentation of the test piece
b	top point		

Figure 1. Typical force-indentation curve [ISO 2008]

This phenomenon is generally known as material relaxation. When the foam is under constant pressure, the deformation is evenly increased and the stress drops. Time strain due to constant stress is called creep.The course of the force response due to the increasing load is shown in Fig. 1. Typically, the curve can be divided into three zones. The first zone with a slight deformation of 10%, there is an almost linear course with higher stiffness. The second zone with a deformation between approximately 10% and 60% is the driving comfort area with the lowest stiffness. The third region with deformation above 60% is characterized by high stiffness and strongly non-linear course.

3   COMPOSITE FOAMS

Considerable efforts have been made to reduce consumption of petroleum products. Several methods of producing natural polyurethanes have been developed [Nurul 2016]. In recent years, PU foams have been made not only from many types of vegetable oils such as soybean, palm, karanja, rapeseed, castor, but also from biowaste such as bamboo, corn, pine bark, kraft lignin and cane [Chang 2015]. In commercial applications, natural polyols can be used as a full or partial replacement of petroleum-based polyols [Desroches 2012], which form the largest volume of polyols used to make PU foams. Despite promising developments in the application of natural oils and their derivatives, their production still faces technical problems like increasing costs, preventing widespread use in flexible foam production. At present, the production of natural-based PU foams is more expensive than the production of foam from petrochemical products [Lligadas 2005]. With technological advances and the inevitable depletion of oil reserves, production of foam from plant ingredients seems to be a possible future solution.
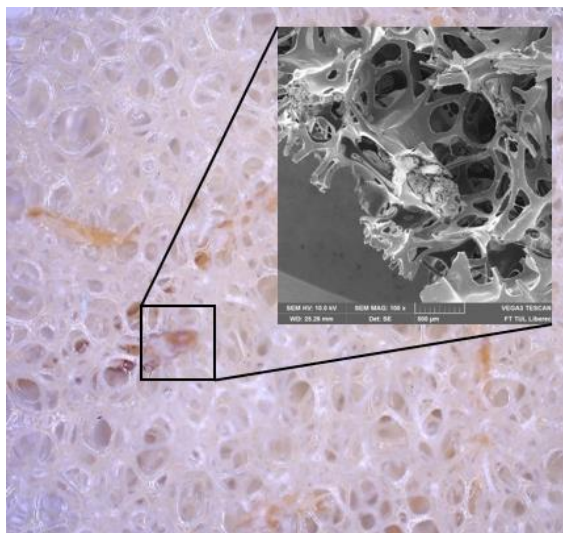

Figure 2. Composite PU foam with coir fibers

Several studies describe the use of natural fibers as reinforcement in PU foams. [Gu 2013] describes the effect of adding cellulose fibers as a filler to both rigid and flexible PU foams. The addition of fibers resulted in an increase of tensile strength and pressure of the rigid foam and an increase in rigidity of the flexible foam. [Shan 2013] researched upon coconut fiber composite foams with regard to vibration damping. After adding 2.5% coconut fibers to a flexible PU foam, an increase in the damping properties of the PU foam was found, but the resonance frequency shifted to higher values compared to pure foam. [Banik 2009] determined the effects of various cellulosic fibrous materials on the formation

of foam structure. The addition of fibers in relatively smaller amount had a significant effect on the structure and the resulting properties of the PU foam. [Chiang 2012] described the development of foam samples with the addition of waste glycerol from the production of biofuels and grass fibers. He concluded that as the amount of fiber increases, the overall density of the composite foam decreases while stiffness decreases. Composite PU foam samples with 5% of fiber reinforcement, having dimensions 100mm x 100mm x 100mm were created. Fig. 2 shows microscopic image of PU foam with coir fibers at 500x magnification.

4   FINITE ELEMENT MODEL

The finite element model of composite PU foam with fibrous reinforcement was created for a brick shaped sample with dimensions 100mm x 100mm x 100mm. First a model of neat PU foam was created without reinforcement. The numerical model shown in Fig. 3 consists of two rigid plates with the test sample placed between them.
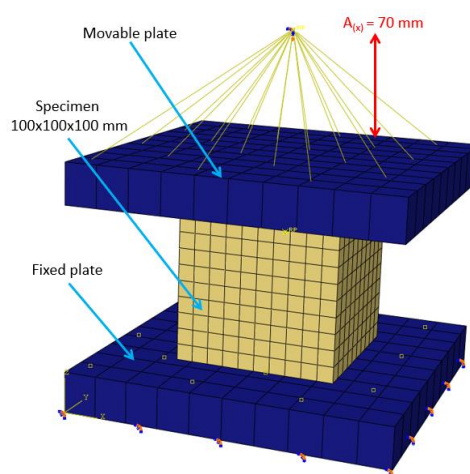

Figure 3. Numerical simulation of compression test

The bottom plate is fixed - motion is prevented in all directions, while the top plate is only allowed to move in the vertical axis where the compression is applied at a speed of 100 mm. min^{-1}. The compression was carried out to 70 % of sample thickness. A friction coefficient of 0.2 was applied to the contact surfaces [Srb 2018]. The PU foam was defined as hyperfoam material in Abaqus. The abaqus hyperfoam [Siranosian 2012, Hibbitt 2013] model is a nonlinear, isotropic material model that is valid for cellular solids with porosity that permits large volumetric changes and is suitable for hyperelastic foams. The model is based on the strain energy function of the form

$$U = \sum_{i=1}^{N} \frac{2\mu_i}{\alpha_i^2} \left[\hat{\lambda}_1^{\alpha_i} + \hat{\lambda}_2^{\alpha_i} + \hat{\lambda}_3^{\alpha_i} - 3 + \frac{1}{\beta_i} \left((J^{el})^{-\alpha_i \beta_i} - 1 \right) \right] \quad (1)$$

where N is a material parameter; μ_i, α_i and β_i are temperature dependent material parameters. The independent variables λ_i are principal stretches and are related to strain in a continuum. The term J^{el} is the elastic volume ratio and is a function of the principal stretches. Parameter β_i is related to the to the Poisson's ratio v_i by the expression

$$\beta_i = \frac{v_i}{1 - 2v_i} \quad (2)$$

The model order N = (1÷6), must be chosen and the material parameters α_i, β_i and μ_i can either be specified, or computed by Abaqus using a least square fit that minimizes error in the computed stress when experimental data is given. The

Poisson's ratio can also be specified or computed. The acceptable experimental data for this model are uniaxial, biaxial and volumetric. Tab. 1 shows numerical simulation parameters.

Part	El. type	El. size [mm]	Number of el.	Friction coef.	Time step [s]
Plate	C3D8R	5	100	0.2	$4.64.10^{-7}$
Foam	C3D8R	1.5	4950	0.2	$4.42.10^{-5}$
Fibers	C3D8R	0.3	4416	0.2	$2.28.10^{-7}$

Table 1. Sample simulation parameters

The material curves were fitted to the curves according to the measured values from a real pure PU foam compression experiment. The geometry resembling the shape of the real fibers of 0.4 mm diameter was created. Then geometry of the foam segment (5mm x 5mm x 20 mm) was created with a cavity corresponding to the dimensions of the fiber. The fibers were connected to foam segments by tie constraint. The individual segments of foam with fiber were assembled into a block of 20mm x 20mm x 20mm. Each segment was rotated at a different angle according to the longitudinal axis. The arrangement of the fibers in foam is shown in Fig. 4.
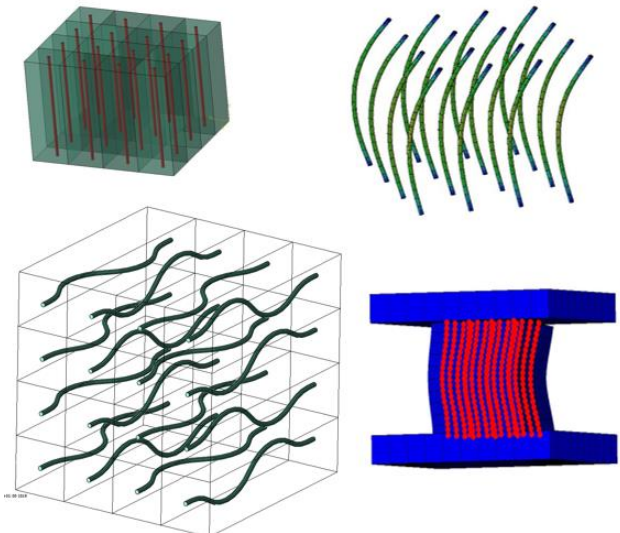

Figure 4. Different arrangement and geometry of fibers

The arrangement and geometry of the fibers was chosen to best match the actual composite sample produced. The sample size was chosen with respect to computational complexity.

Fig. 5 shows a side view of the arranged fibers in a 20mm x 20mm x 20 mm non-deformed composite foam block. It can be seen from the arrangement that there are minimal gaps filled with PU foam between individual fibers. In the beginning of the compression only the PU foam is deformed and the influence of the fibers is not significant. After around 20 % of compression, the reinforcing effect of the fibers starts to appear gradually. During further compression, the undulated fibers tend to straighten, which is prevented by tight bonding of the PU foam and fibers. The fibers are subjected to torsion and bending, and the foam is locally deformed, resulting in increased stiffness of the composite foam. With further deformation, this effect continues to increase, with the individual fibers almost in contact, where the PU foam is compressed to a high level between them and behaves as very stiff. Fig. 6 shows the result of simulating the deformed fibers at 70% compression of the composite foam. Fig. 7 shows values obtained by experimental compression of a PU foam sample and numerical simulations

made using the Mooney - Rivlin model and the Ogden models for N = 1 and 2. By setting the corresponding geometry and material properties of the fibers, a very good agreement of the load characteristic curve was achieved. The load characteristic thus obtained will be used as an input material parameter to simulate the compression of the entire foam part of the seat.
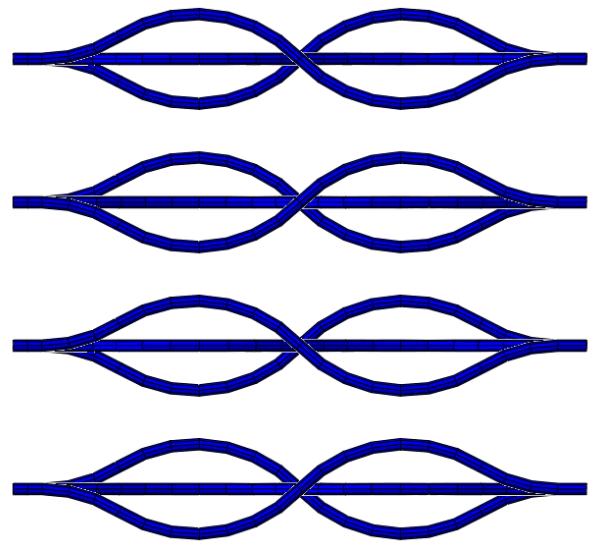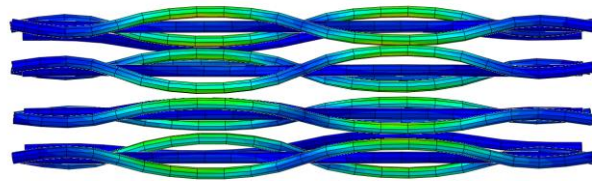

Figure 5. Side view of arranged fibers

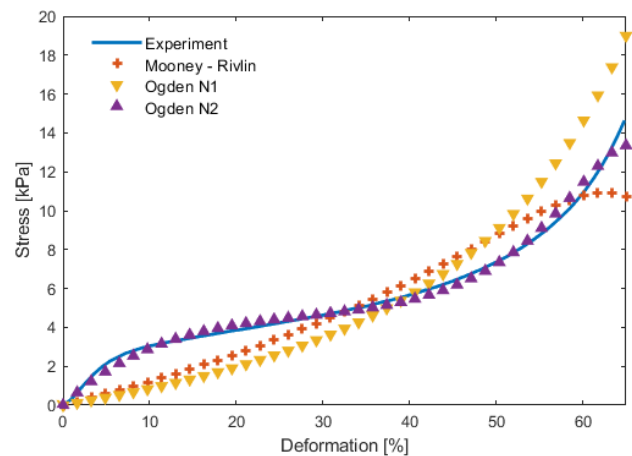**Figure 6.** Side view of arranged fibers under 70% deformation

Figure 7. Comparison of stress-strain curves of numerical simulation and real experiment.

Part	El. type	El. size [mm]	Number of el.	Fric. coef.	Time step [s]
Circular ind.	C3D8R	10	496	0.2	$9.53.10^{-7}$
Body sh. ind.	S3R	5	5628	0.2	$6.31.10^{-7}$
Cushion	C3D4	8	21324	0.2	$6.73.10^{-6}$

Table 2. Cushion simulation parameters

Model simulations of a sample of a car seat cushion made of low density composite foam with natural fibers were created. The mesh of finite elements of the cushion was made of 3D elements of tetrahedrons. The circular indentor was created from 3D hexahedron elements and a body shape indentor from 2D Shell elements. Tab. 2 shows simulation parameters of car seat cushion and indetors. The boundary conditions have been defined so that the nodes of the lower part of the cushion that are in contact with rigid car seat frame are fixed, constraints $U_i = 0$, $R_i = 0$ was applied. A circular indentor and an indentor based on the shapes of the human body were pressed into the car seat cushion. The position of the indentor and the compression parameters were determined based on discussion with the car seat manufacturer. A contact with a coefficient of friction of 0.2 was applied between the seat cushion and the indentor. Due to the uneven height of the cushion material, which ranges from 50 to 80 mm, the indentor indentation depth of 35 mm was chosen, corresponding to 70% of the cushion height at the lowest point. Arrangement of simulation can be seen on Fig. 8 which has appropriate conditions as experimental measurement (Fig. 9).
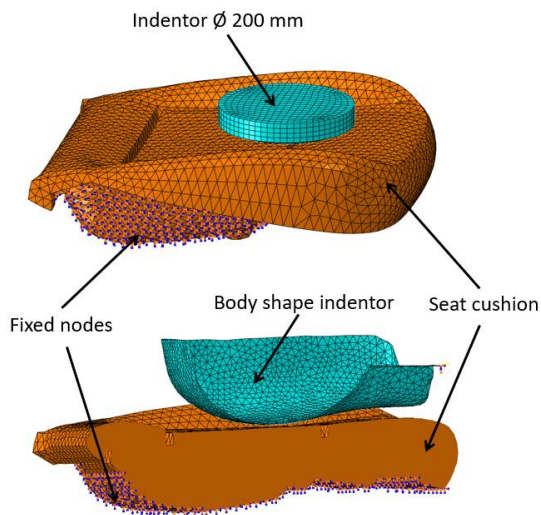

Figure 8. Numerical model of compression car seat cushion with different types of indentors
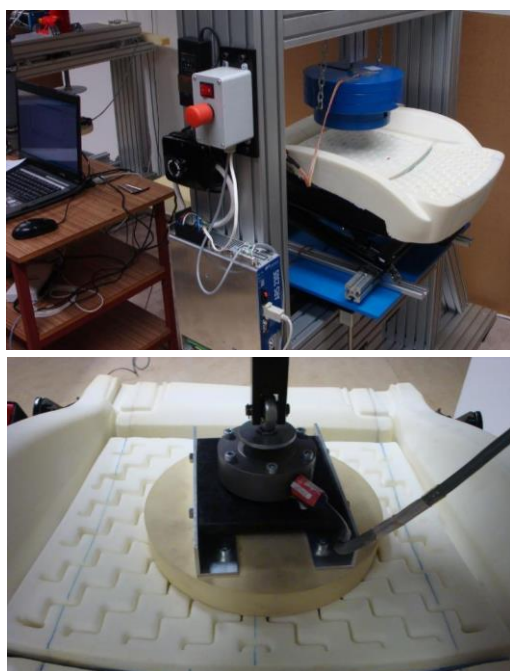

Figure 9. Experimental measurement of compression in car seat cushion with different types of indentors

Contact can be defined as contacting two surfaces that interact as contact pairs or a self-contact that interacts with itself. In this case of static compression of the sample, it is the contact of two bodies. Abaqus allows several contact formulations, according to the method of discretizing the contact surfaces and according to the classification of the relative movement of the contact surfaces. In this case, surface to surface discretization was chosen. This approach considers both the master and slave shapes in the contact condition region. Slave surface penetration is possible by master surface nodes, but slave nodes cannot penetrate master surface. The surface to surface approach provides a smoother stress distribution. Larger penetrations rarely occur, generally providing more accurate results than the node to surface algorithm, but it is more computationally complicated. First, it is necessary to determine the master surface and the slave surface. For the selection of the master surface there are several recommendations: it should be a larger area, a surface with a higher stiffness and a surface with a coarser mesh. In the case of compressing the cushion, the master surfaces were the indentor and the slave surface was the compressed sample.

5   RESULTS

A car seat cushion made of composite foam with reinforcing fibers was created. This cushion was subjected to indentor compression and the results were compared with a conventional neat PU foam seat cushion.
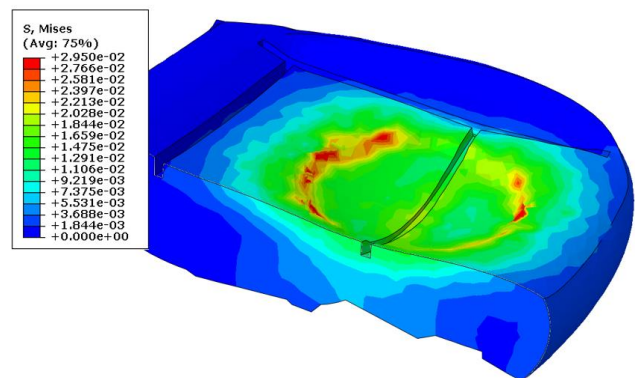

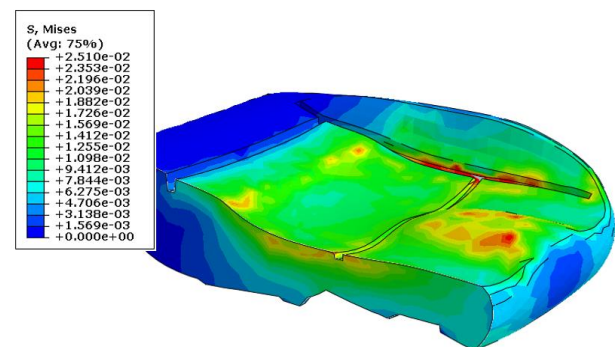**Figure 10.** Stress distribution on car seat cushion compressed by circular indentor

Figure 11. Stress distribution on car seat cushion compressed by human body shaped indentor

A numerical simulation corresponding to real experiments was created, for neat PU foam and foam reinforced with natural fibers. Fig. 10 and 11 show results of stress distribution of compressed seat cushion by two types of indentors. From the results of model simulations with circular indentor creating compression up to 35 mm, it can be seen that the deformation of the foam in directions perpendicular to the direction of

compression leads to an even distribution of contact pressure. There is an almost even stress distribution in both the neat PU foam seat cushion sample and the reinforced foam. The contact pressure from the circular indentor on the neat foam cushion sample is 19 kPa, while that on the reinforced foam is about 12% higher, i.e. 21.3 kPa. In the case of the body shape indentor, the contact pressure on the neat foam cushion sample is 15.2 kPa, while that on the reinforced foam is about 9% higher, i.e. 16.6 kPa. Yet it is a lower value compared to the circular indentor. The stress shows a value of 24.3 kPa for neat PU foam and 29,4 kPa for reinforced foam from a circular indentor load and 20.4 kPa for neat PU foam and 25.2 kPa for reinforced foam under load from the body shaped indentor. It follows that the distribution and size of the contact pressure is influenced by the shape of the load geometry and the characteristic stiffness of the material structure. A complete comparison of the force response course for simulations and experiments was performed using neat foam and reinforced foam while loading by two types of indentors. The results shown in Fig. 12 show a very good agreement of simulations with experiments. The largest deviation of simulation from the experiment was 11% as shown by the compression of the reinforced foam cushion by the indentor of the human body shape. For other experiments and simulations there were deviations at maximum 5%.
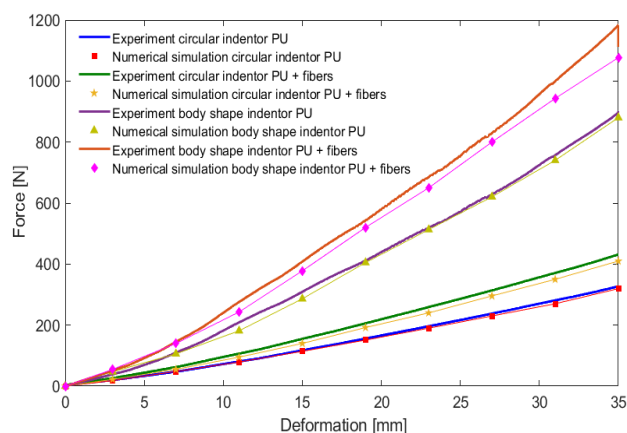

Figure 12. Stress distribution on car seat cushion compressed by human body shaped indentor

6   CONCLUSIONS

Numerical simulations were performed to study and compare mechanical properties between standard PU foam and low-density composite foam with coir. From the results it was determined that the compression curves are similar, wherein the fiber reinforcement increases stiffness and compression resistance. The resulting dependence of force on deformation is in good agreement with the experiments. Subsequently, the model can be used to express, for example, stiffness and energy dissipation in a PU foam sample and in a sample of low-density composite foam reinforced with coir. Composite foam with fibrous reinforcement shows superior tensile behavior because PU foam is not capable to transmit tensile stresses. While PU foam is under tensile stress, the stiffness will be very high with very low deformability. It means that lower deformation and force cause a tearing of the cell structure. If the torn foam is further stressed, complete destruction/failure occurs. This is especially important for assembling of car seat, such as inserting a seat foam, backrest, or headrests. The numerical simulations intended for design of whole composite car seat cushion were developed. The results were successfully used for study and comparison of deformation and stress distribution as well as contact pressure.

REFERENCES

[Banik 2009] Banik, I. and Sain, M.M. Water-blown soy polyol based polyurethane foams modified by cellulosic materials obtained from different sources. Journal of Applied Polymer Science, 2009, Vol 112, Issue 4, pp 1974-1987, ISSN 1097-4628

[Chang 2015] Chang, L. et al. Effect of mixing conditions on the morphology and performance of fiber-reinforced polyurethane foam. Journal of Cellular Plastics, 2015, Vol. 51, Issue 1, pp 103-119, ISSN 1530-7999

[Chiang 2012] Chiang, C.C. Synthesis of green polyurethane foam using waste glycerol and hay fibers. California State University, Long Beach, 2012

[Desroches 2012] Desroches, M. et al. From vegetable oils to polyurethanes: synthetic routes to polyols and main industrial products. Polymer Reviews, 2012, Vol 52, Issue 1, pp 38-79, ISSN 1558-372

[Emori 2020] Emori, K., Fushimi, S., Miura, T., Yonezu, A. FEM simulation of polymeric foam with random pore structure: Uniaxial compression with loading rate effect, Polymer testing, 2020, Vol. 82, Issue 26, pp 1-7, doi: 10.1016/j.polymertesting.2019.106303

[Fahy 2015] Fahy, R. and Thompson, D. Fundamentals of Sound and Vibration. CRC Press, 2015, ISBN 9780415562102

[Griffin 2004] Griffin, M.J. Handbook of Human vibration. University Soupthamton, UK, MCSLimited, 2004, ISBN 0-12-303041-2

[Gu 2013] Gu, R. et al. A feasibility study of polyurethane composite foam with added hardwood pulp. Industrial Crops and Products, 2013, Vol. 42, pp 273-279, ISSN 0926-6690

[Hibbitt 2013] Hibbit et al. ABAQUS/CAE 6.13 User's Manual, Dassault Systemes, 2013

[ISO 2008] ISO-2439 Flexible cellular polymeric materials - Determination of hardness (indentation technique). Geneva, ISO copyright office, 2008.

[Kamp 2012] Kamp, I. The influence of car-seat design on its character experience. Applied Ergonomics, 2012, Vol. 43, Issue 2, pp 329-335, ISSN 0003-6870

[Lligadas 2005] Lligadas, G. et al. Synthesis and characterization of polyurethanes from epoxidized methyl oleate based polyether polyols as renewable resources. Journal of Polymer Science Part A: Polymer Chemistry, 2005, Vol 44, Issue 1, ISSN 1099-0518

[Marvi-Mashhadi 2020] Marvi-Mashhadi, M., Lopes, C.S., LLorca, J. High fidelity simulation of the mechanical behavior of closed-cell polyurethane foams. Journal of the Mechanics and Physics of Solids, 2020, Vol 135, pp 1-14, doi: 10.1016/j.jmps.2019.103814

[Nurul 2016] Nurul, H. Structure property performance of natural palm olein polyol in the viscoelastic polyurethane foam. Journal of Cellular plastics, 2016, Vol 53, Issue 1, pp 65-81, ISSN 1530-7999

[Petru 2017] Petru, M. and Novak, O. Measurement and Numerical Modeling of Mechanical Properties of Polyurethane Foams. Book Chapter n.4: Aspects of Polyurethanes, 2017, doi: 10.5772/intechopen.69700

[Shan 2013] Shan, C.W. et al. Improved Vibration Characteristics of Flexible Polyurethane foam via Composite Formation. International Journal of Automobive and Mechanical Engineering, 2013, Vol 7, pp 1031-1042, ISSN 2229-8649

[Siranosian 2012] Siranosian, A. and Stevens R. Developing an Abaqus *HYPERFOAM Model for M9747 (4003047) Cellular Silicone Foam. Report AC52-06NA25396, Los Alamos National Lab, 2012

[Srb 2018] Srb, P. and Petru, M. Numerical simulation of reinforced polyurethane foam. Experimental Stress Analysis - 56th International Scientific Conference, EAN 2018 - Conference Proceedings, pp. 381-386, ISBN 978-802704062-9

[Szycher 2017] Szycher, M. Szychers handbook of polyurethanes. CRC Press, 2017, ISBN 9781138075733

[Valentini 2012] Valentini, P. Modeling human spine using dynamic spline approach for vibrational simulation. Journal of Sound and Vibration, 2012, Vol. 331, Issue 26, pp 5895-5909, ISSN 0022-460X

CONTACTS:

Ing. Pavel Srb, Ph.D.
Institute for Nanomaterials, Advanced Technologies and Innovation, Technical University of Liberec
Studentska 2, Liberec 461 17, Czech Republic
+420 728 338 561, pavel.srb@tul.cz, https://cxi.tul.cz/